Negative charge-transfer gap and even parity superconductivity in Sr_2RuO_4

Sumit Mazumdar
Department of Physics, University of Arizona, Tucson, Arizona 85721, USA;
Department of Chemistry and Biochemistry, University of Arizona, Tucson, Arizona 85721, USA;
and College of Optical Sciences, University of Arizona, Tucson, Arizona 85721, USA

(Received 17 February 2020; revised manuscript received 27 April 2020; accepted 29 May 2020; published 23 June 2020)

A comprehensive theory of superconductivity in Sr_2RuO_4 must simultaneously explain experiments that suggest even-parity superconducting order and yet others that have suggested broken time-reversal symmetry. Completeness further requires that the theory is applicable to isoelectronic Ca_2RuO_4, a Mott-Hubbard semiconductor that exhibits an unprecedented insulator-to-metal transition which can be driven by very small electric field or current, and also by doping with very small concentration of electrons, leading to a metallic state proximate to ferromagnetism. A valence transition model, previously proposed for superconducting cuprates [Mazumdar, Phys. Rev. B **98**, 205153 (2018)], is here extended to Sr_2RuO_4 and Ca_2RuO_4. The insulator-to-metal transition is distinct from that expected from the simple melting of the Mott-Hubbard semiconductor. Rather, the Ru ions occur as low spin Ru^{4+} in the semiconductor, and as high spin Ru^{3+} in the metal, the driving force behind the valence transition being the strong spin-charge coupling and consequent large ionization energy in the low charge state. Metallic and superconducting ruthenates are thus two-component systems in which the half-filled high spin Ru^{3+} ions determine the magnetic behavior but not transport, while the charge carriers are entirely on the layer oxygen ions, which have an average charge of -1.5. Spin-singlet superconductivity in Sr_2RuO_4 evolves from the correlated lattice-frustrated $\frac{3}{4}$-filled band of layer oxygen ions alone, in agreement with quantum many-body calculations that have demonstrated enhancement by electron-electron interactions of superconducting pair-pair correlations uniquely at or very close to this filling [Gomes, Wasanthi De Silva, Dutta, Clay, and Mazumdar, Phys. Rev. B **93**, 165110 (2016); Wasanthi De Silva, Gomes, Mazumdar, and Clay, Phys. Rev. B **93**, 205111 (2016)]. Several model-specific experimental predictions are made, including that spin susceptibility due to Ru ions will remain unchanged as Sr_2RuO_4 is taken through superconducting T_c.

DOI: 10.1103/PhysRevResearch.2.023382

I. INTRODUCTION

Sr_2RuO_4 has long been thought of as a chiral spin-triplet superconductor, with orbital parity $p_x \pm ip_y$ [1]. This viewpoint has recently been challenged by multiple experiments [2–8] that are beginning to lead to a thorough reexamination of earlier experiments or their interpretations and theories. A few investigators have even suggested that the superconducting pairing might have even parity, likely d wave [6,9]. In the present theoretical paper, which is an extension of a valence transition model [10] recently postulated for superconducting cuprates and doped barium bismuthate, $(Ba, K)BiO_3$, I posit that the peculiarities observed in Sr_2RuO_4 and the isoelectronic Ca_2RuO_4 should not be considered in isolation, but that the unconventional behaviors of all these superconducting perovskite oxides, along with the pseudogaplike features [11–13] observed in electron-doped Sr_2IrO_4, can be understood within a common theoretical model. The key theoretical features of this theory are valence transition and negative charge-transfer gap, which in all cases are driven by a unique property common to the materials of interest: the essential cation in each material has a strong tendency to have true ionicity lower than the formal ionicity by a full integer unit. This is a strong correlations effect that is missed in band or first-principles calculations, which invariably find a single phase with mixed valence as opposed to distinct phases with nearly integer valences.

It is useful to point out here that the concept of valence transition in systems consisting of donor and acceptor components is widely accepted in the context of pressure, temperature, and light induced neutral-to-ionic transition in quasi-one-dimensional mixed-stack organic charge-transfer solids [14–16]. The concept of quantum critical valence fluctuation in heavy fermions [17] is qualitatively similar. In the superconducting oxides the consequence of valence transition is an insulator-to-metal transition (IMT) where the metallic state is different from that arising from simple "doping" or "self-doping" of the semiconductor, as has been assumed until now. Within the proposed model the insulating phase has the usual $M^{n+}(O^{2-})_2$ intralayer unit-cell composition, but the true (as opposed to formal) ionic composition in the pseudogap and metallic states is $M^{(n-1)+}(O^{1.5-})_2$. The pseudogap state (wherever applicable) and the "normal" state from which

superconductivity (SC) emerges thus consist of a strongly correlated oxygen (O) band in which nearly half the oxygens (as opposed to a few) have ionicities O^{1-}. The cations in their true ionicities are either closed shell or exactly half filled and play no role in SC.

The negative charge-transfer gap model is arrived at from heuristic arguments as opposed to direct computations, as the sheer number of many-body interactions and parameters that would enter such computations are enormously large. The relative magnitudes of the different parameters that would enter a complete theoretical model are known, however, which allows making the physical arguments for the transition. This approach is counter to existing theoretical approaches to Sr_2RuO_4, but as in the previous work [10] it will be shown that (nearly) all the experimental observations that are difficult to explain within any other single theory can be explained relatively easily once the fundamental premise is accepted. The validity of the model can therefore be tested only by comparing theoretically arrived at conclusions against existing experiments as well as new experiments that are performed to test predictions of the theory. It then becomes necessary to list the full set of experiments that any theory that claims to be comprehensive should be able to explain at least qualitatively. This is the approach that was taken in the earlier work on the cuprates [10] and is taken here for Sr_2RuO_4 and Ca_2RuO_4.

In the next section I list what I believe are the most challenging observations, including apparent contradictions, in (i) Sr_2RuO_4 and (ii) the isoelectronic Mott-Hubbard semiconductor Ca_2RuO_4, which exhibits dramatic IMT induced by current [18,19] and electron doping [20], as well as exotic behavior in the nanocrystal form [21]. Existing theories of Sr_2RuO_4 largely attempt to determine the superconducting symmetry of the material while ignoring the highly unusual behavior of Ca_2RuO_4. The approach here is to treat both systems on an equal footing. Following this I briefly present in Sec. III the theory of what I term as the type-I negative charge-transfer gap, as observed in doped cuprates, $BaBiO_3$ and (Ba, K)BiO_3, and doped Sr_2IrO_4 in an octahedral environment. Although much of this has already been presented in the earlier work [10], it is necessary to repeat this briefly here to point out the unique common feature shared by Cu^{1+}, Bi^{3+}, Ir^{3+} in the octahedral environment, and Ru^{3+}. It is this shared feature that is the driver of an unusual IMT in these perovskite oxides. Section IV discusses the physical mechanism behind the valence transition that drives what I term as the type-II negative charge-transfer gap in Sr_2RuO_4. Section V shows how all the experiments listed in Sec. II, in particular, (i) spin-singlet even-parity SC and the confusing experimental observations on time-reversal symmetry breaking in Sr_2RuO_4 and (ii) the current and electron-doping induced metallicity in Ca_2RuO_4 and perhaps even the SC claimed to have been observed in this system, *can be simultaneously understood within the theoretical model*. Finally in Sec. VI I make experimentally testable predictions on Sr_2RuO_4 that are completely specific to the negative charge-transfer gap model. Section VII presents the conclusions, focusing in particular on the unique features of the correlated $\frac{3}{4}$-filled band.

II. THEORETICAL CHALLENGES

A. Experimental puzzles: Sr_2RuO_4

1. T_c enhancement under uniaxial pressure

The superconducting critical temperature T_c in Sr_2RuO_4 crystals is strongly enhanced upon the application of uniaxial pressure along the [100] direction [3–5], even as hydrostatic pressure suppresses T_c. Starting from the ambient pressure value of 1.5 K, T_c reaches a peak value of 3.4 K at uniaxial compression of 0.6%, following which T_c decreases again. Based on band-structure calculations it has been suggested the peak in T_c corresponds to the compression at which the Fermi level crosses the van Hove singularity [5]. Theoretically predicted splitting of the transition temperatures due to separate p_x and p_y components was not observed. The superconducting transition at the maximum T_c is very sharp, allowing precise determinations of the upper critical fields for magnetic fields both along the intraplane [100] direction ($H_{c2||a}$) as well as perpendicular to the plane ($H_{c2||c}$). While $H_{c2||c}$ is enhanced by more than a factor of 20 relative to unstrained Sr_2RuO_4, in-plane $H_{c2||a}$ is enhanced by only a factor of 3. Importantly, for the spins lying in the [two-dimensional (2D)] plane, neither orbital limiting nor Pauli limiting should apply to $H||a$, and $H_{c2||a}/H_{c2||c}$ should be infinite within the existing spin and orbital characterization of the superconducting state. *The observed ratio of only about 3 in the strained material casts severe doubts about the chiral p-wave symmetry.*

In view of what follows in Sec. IV, it is pointed out here that strong pressure induced enhancement of T_c is also found in Ce-based heavy fermion superconductors, and is ascribed to critical valence fluctuations by some investigators [17].

2. ^{17}O NMR

The earlier experiment that had given the most convincing evidence for triplet SC was based on the measurement of the O-ion Knight shift as a function of temperature [22]. No change in spin susceptibility was detected as the sample was taken through the critical temperature T_c. Luo *et al.* [7] and Pustogow *et al.* [8] have repeated the ^{17}O NMR measurements in uniaxially compressed Sr_2RuO_4 for different strain levels [3–5], inclusive of the complete range of $T_c = 1.5$–3.4 K. Reduction in the Knight shift, and therefore drop in the spin susceptibility, have been found for all strains, including for the unstrained sample [8]. Most importantly, *the NMR study finds no evidence for a transition between different symmetries.* The experiment conclusively precludes $p_x \pm ip_y$ triplet pairing, and leaves open the possibilities of helical triplet pairings, spin-singlet d_{xy} or $d_{x^2-y^2}$ pairings, and chiral d-wave pairing.

3. Possible breaking of time-reversal symmetry

Muon-spin rotation [23] and magneto-optic polar Kerr rotation [24] measurements had suggested that time-reversal symmetry is broken upon entering the superconducting state. This conclusion has been contradicted by the observation that the Josephson critical current is invariant under the inversion of current and magnetic fields [25]. It is relevant in this context that the polar Kerr effect is also seen in hole-doped

cuprates inside the pseudogap, and while originally this was also ascribed to time-reversal symmetry breaking it has been later ascribed to 2D chirality [26]. Recent muon relaxation experiments on uniaxially stressed Sr_2RuO_4 have found that the onset temperatures of time-reversal symmetry breaking T_{TRSB} and superconducting T_c are different [27]. The authors also found magnetic order in Sr_2RuO_4 under high stress, but ignore this, and ascribe the difference between T_{TRSB} and T_c to two-component SC. Within the existing Ru-centric theories of SC this is the only possibility. Within the negative charge-transfer gap model T_{TRSB} is associated with magnetism involving the Ru ions and T_c is associated with the O ions (see Sec. V).

4. Magnetocaloric and thermal conductivity measurements

Magnetocaloric measurements have found that the superconductor-to-metal transition in the unstrained material at $T \simeq 0.5T_c$ is first order, indicating that the pair breaking is Pauli limited, i.e., pairing is of spin-singlet type [28]. Among the symmetries not precluded by the ^{17}O NMR experiment [8] the helical triplet orders and the chiral d-wave order have horizontal nodes while the d_{xy} and $d_{x^2-y^2}$ orders have vertical nodes. Recent thermal conductivity measurements have found evidence for vertical line nodes consistent with d-wave pairing [6].

B. Experimental puzzles: Ca_2RuO_4

Replacement of Sr with Ca generates the isoelectronic Ca_2RuO_4 as well as the "doped" compounds $Ca_{2-x}Sr_xRuO_4$, $0 \leqslant x \leqslant 2$. Ca_2RuO_4 is an antiferromagnetic semiconductor with energy gap between 0.2 and 0.4 eV at low temperatures [29–32]. Ru ions in this compound have ionicity +4 and are in the low spin state, with $4d$ orbital occupancy t_{2g}^4. Néel temperature of 113 K and paramagnetic semiconductor to paramagnetic metal transition at ≈360 K show that the system is a Mott-Hubbard semiconductor. The mechanism of the Mott-Hubbard IMT remains controversial but one popular mechanism involves increased d_{xy} occupancy to up to two electrons due to Jahn-Teller distortion, with Hund's rule coupling leading to one electron each in the d_{xz} and d_{yz} orbitals [31,33,34]. The half-filled nature of the d_{xz} and d_{yz} bands then leads to Mott-Hubbard semiconducting behavior. The Mott-Hubbard transition is accompanied with structural distortions involving tilts and rotations of the RuO_6 octahedra, with the layer (apical) Ru-O bonds becoming shorter (longer) in the metallic phase (the semiconducting antiferromagnetic and the metallic phases are commonly labeled as S and L, respectively) [30]. Similar structural changes are also seen in pressure induced IMT transition, where the metallic state is found to be proximate to ferromagnetism [35]. "Doping" induced IMT occurs in $Ca_{2-x}Sr_xRuO_4$ for $x > 0.2$. Importantly, the high-temperature metallic phase in Ca_2RuO_4, the paramagnetic metallic phase $0.5 \leqslant x \leqslant 1.5$, and the $x = 2$ phase pure Sr_2CuO_4 are all structurally different. Latest experiments have found completely different IMT that has not been seen so far in any other Mott-Hubbard semiconductor, as described below.

1. Current induced IMT

An unprecedented electric-field induced IMT, with a lower threshold field of 40 V/cm, tiny compared to the known semiconducting gap of 0.2–0.4 eV, has been found in Ca_2RuO_4 [18,19]. Strong current induced diamagnetism, the origin of which is not understood, appears in the semimetallic state reached with a current density as low as 1 A/cm^2 [36]. The IMT is not due to Joule heating, as evidenced by Raman spectroscopy [37] and the nucleation of the metallic phase at the negative electrode [38]. The crystal structure of the current induced semimetallic state is different from the equilibrium state reached by applications of temperature, pressure, or strain [39]. The rapid suppression of the antiferromagnetic order and resistance even at the smallest currents is accompanied by strong lattice distortions [38–40] (Ref. [40], however, does not find diamagnetism). The very strong "coupling" between the current and lattice structure has led to the suggestion that the t_{2g} orbital occupancies of Ru^{4+} ions in the semiconductor and the current-carrying state are different [40].

2. IMT induced by La substitution

There exist remarkable yet hitherto unnoticed similarities between IMT induced by current and electron doping by substitution of La for Ca. The ionic radii of Ca^{2+} (1.00 Å) and La^{3+} (1.03 Å) are nearly equal. The consequences of La-substitution are more dramatic than Sr substitution, even though Sr_2RuO_4 is isoelectronic with Ca_2RuO_4 [20]. For x as small as 0.005 in $Ca_{2-x}La_xRuO_4$, the temperature at which the IMT occurs drops by nearly 80 K and resistance decreases by two orders of magnitude throughout the measured temperature range. The system is also ferromagnetic below 125 K. For $x = 0.1$, the system is metallic down to 2 K and the resistance drops to 10^{-4} Ω cm from ≈10^9 Ω cm at $x = 0$. The IMT is accompanied by large increases in Pauli paramagnetic susceptibility and the coefficient γ of electronic specific heat (γ increases from 16 to 90 mJ/mole K^2 from $x = 0.01$ to 0.035) as well as large structural distortions. The unusually large increase in conductivity with the slightest of electron doping and under very small electric fields both indicate that *the ground state of the undoped compound is very close to an exotic instability*.

3. Possible coexistence of SC and ferromagnetism

A very recent work on nanofilm (as opposed to bulk) crystals of Ca_2RuO_4 has reported an even more perplexing phenomenon, possible coappearance of ferromagnetism and superconducting order [21]. The nanofilm crystals had the same L phase structure as metallic Ca_2RuO_4 as opposed to the S structure in the bulk antiferromagnetic phase. SC seems to appear within a ferromagnetic phase with $T_{Curie} \sim 180$ K. The authors find a diamagnetic component within the ferromagnetic phase above the superconducting T_c that is larger than that found in Ref. [36], and ascribe this to preformed Cooper pairs [21]. The diamagnetism is enhanced by ferromagnetism in some of the samples, which led to the conclusion of coexistence of SC and ferromagnetism. The authors ascribe the observations to chiral p-wave SC, which would, however, contradict the ^{17}O-NMR experiment in Sr_2RuO_4 [8]. I point

out in Sec. III that these experiments are reminiscent of the appearance of SC in undoped thin-film T' cuprates [41].

C. Summary

To summarize, any theory of Sr_2RuO_4 must simultaneously explain the apparent contradictions between the ^{17}O NMR experiments [7,8] and the muon experiments [23,27], and also between experiments that find preservation [25] as well as breaking [23,27] of time-reversal symmetry. Proper understanding of the current [18,19,36,38–40] and electron-doping [20] induced IMTs in Ca_2RuO_4, *including of the similarities in the observations in the two cases*, are essential, as the detailed mechanisms of these transitions likely reveal the origin of the difference between Ca_2RuO_4 and Sr_2RuO_4. Band calculations ascribe the difference to lattice distortions; however, the distortions themselves can be *consequences* of different Madelung stabilization energy contributions to the total energies of Ca_2RuO_4 and Sr_2RuO_4 (see Sec. V), given the large differences in ionic radii of Ca^{2+} and Sr^{2+}. The proximity of ferromagnetism to the superconducting state (or even their coexistence in nanofilm Ca_2RuO_4 [21]) is suggested from multiple experiments. A consistent explanation of all of the above features within a single theory is currently lacking.

III. CUPRATES, BISMUTHATE, AND IRIDATES

The central postulate of the present paper is that the peculiarities observed in Sr_2RuO_4 should not be considered in isolation, as equally perplexing mysteries persist with the other perovskite superconductor cuprates and (Ba, K)BiO_3, and in the pseudogaplike state [11–13] in electron-doped Sr_2IrO_4. I argue in this subsection that the failure to arrive at a comprehensive theory in every case stems from focusing on *cation-centric Hamiltonians* (for, e.g., the single-band Hubbard model for cuprates). In the following I first list the experiments in the cuprates, (Ba, K)BiO_3 and Sr_2IrO_4, that most strongly argue against cation-centric Hamiltonians. Following this a brief presentation of the theory behind negative charge-transfer gap [10] in these systems is presented.

A. The need to go beyond cation-centric models: Experiments

(i) The simultaneous breaking of rotational and translational symmetries in the hole-doped T-phase cuprates, accompanied by intra-unit-cell O-ion inequivalency [42–45], illustrate most strongly the need to incorporate the O ions explicitly in any starting theoretical description of the cuprates. With the T' cuprates, the most peculiar features are (i) the very robust antiferromagnetism in the "usual" electron-doped materials [46]; (ii) the appearance of SC at *zero doping* nevertheless in specially prepared thin-film samples, with T_c higher than the maximum T_c in the usual materials [41] (see also discussion of possible SC in undoped nanocrystals of Ca_2RuO_4 in Sec. II B); and (iii) charge order with *nearly the same periodicity as the hole-doped cuprates* [47,48]. Taken together, these observations present the following conundrum. On the one hand, inequivalent O ions in the hole-doped compounds in the charge-ordered state from which the superconducting states emerge require that the O ions are included in any attempt to construct a comprehensive theoretical model. On the other, the apparent symmetry between the hole- and electron-doped compounds (in so far as SC is concerned) *requires* explanation within a single-band model, since electron-hole symmetry is absent within multiband models.

(ii) Negative charge-transfer gap in $BaBiO_3$ is already recognized. The semiconducting gap in undoped $BaBiO_3$ within traditional cation-centric models [49] had been ascribed to a charge-density wave (CDW) consisting of alternate Bi^{3+} and Bi^{5+} ions. SC in $Ba_{1-x}K_xBiO_3$ within these models emerges from doping the parent Bi-based CDW. Recent theoretical and experimental demonstrations [50,51] of the occurrence of Bi ions exclusively as Bi^{3+} show convincingly that the existing theories of SC are simplistic. *There is also no explanation of the limitation of SC* [50,52] *to K concentration* $0.37 \leqslant x \leqslant 0.5$ *in* $Ba_{1-x}K_xBiO_3$, an issue to which we return later.

(iii) Sr_2IrO_4 has attracted strong attention in recent years as an effective square lattice Mott-Hubbard insulator. The active layer consists of IrO_2 unit cells with nominally tetravalent Ir^{4+}. The d-electron occupancy is t_{2g}^5 as a consequence of large crystal-field stabilization energy (CFSE). The t_{2g} orbitals are split by spin-orbit coupling into lower twofold degenerate total angular momentum $J_{\rm eff} = \frac{3}{2}$ levels and an upper nondegenerate narrow $J_{\rm eff} = \frac{1}{2}$ level [53]. Occupancy of the latter by a single unpaired electron explains the Mott-Hubbard–like behavior of undoped Sr_2IrO_4. Remarkable similarities [11–13,54] are found between hole-doped cuprates in the pseudogap phase and and electron-doped Sr_2IrO_4. Following the vanishing of the Mott-Hubbard gap at ≈5% doping there appears a d-wave-like gap in the nodal region, with strong deviation in the antinodal region, where the gap is much larger [13], exactly as in the cuprates [55]. Theoretical attempts to explain these observations borrow heavily from the single-band Hubbard model description for cuprates, which, we have pointed out, is at best incomplete.

B. The need to go beyond cation-centric models: Theory

It is useful to point out a crucial recent theoretical development. Convincing proof of the absence of SC in the weakly doped 2D Hubbard Hamiltonian with nearest-neighbor-only hoppings has been found from a comprehensive study that used two different complementary many-body techniques [56]. While Ref. [56] leaves open the possibility that SC might still appear within a more complex Hubbard model with next-nearest-neighbor (NNN) hopping, calculations of the Hubbard U dependence of superconducting pair-pair correlations in triangular lattices preclude SC in the carrier concentration range 0.75–0.9 [57], which has been thought to be appropriate for cuprates.

C. Type-I negative charge-transfer gap: Cations with closed shells

The traditional approach to arriving at phenomenological minimal Hamiltonians for complex oxides *assumes* that the nominal and true charges (ionicities) of the active cation and the O ions are the same. The known example of $BaBiO_3$ (see above) already indicates that this can be incorrect. Physical understanding of the distinction between true versus formal

charge is best obtained within strongly correlated ionic models [16,58–60]. What follows merely requires small electron or hole hoppings between the central cation (Bi in $BaBiO_3$) and the O anion, relative to the largest many-electron interactions. For any cation M that can exist in two different valence states M^{n+} and $M^{(n-1)+}$, the true ionic charge of the oxide is determined by the inequality [10]

$$I_n + A_2 + \Delta E_{M,n} + \Delta(W) \gtrless 0 \qquad (1)$$

where I_n is the energy of the nth ionization ($M^{(n-1)} \rightarrow M^{n+} + e$) and A_2 is the second electron affinity of O ($O^{1-} + e \rightarrow O^{2-}$). Here $\Delta E_{M,n} = E_{M,n} - E_{M,n-1}$, where $E_{M,n}$ is the Madelung energy of the solid with the cation charge of $+n$. $\Delta(W) = W_n - W_{n-1}$, where W_n and W_{n-1} are the gains in total one-electron delocalization (band) energies of states with cationic charges $+n$ and $+(n-1)$, respectively. I_n and A_2 are positive, while $\Delta E_{M,n}$ is negative. Note that (i) W_n and W_{n-1} are both negative and (ii) for a cation charge of $+n$ there are very few charge carriers, while for cation charge $+(n-1)$ a large fraction of the O ions (nearly half) are O^{1-} and the number of charge carriers is far larger, making $\Delta(W)$ positive. The two largest quantities in Eq. (1), I_n and $\Delta E_{M,n}$, have opposite signs and magnitudes several tens of eV or even larger (see below), and are many times larger than A_2 and $\Delta(W)$, which are both a few eV. This introduces the possibility of distinct quantum states with nearly integer valences, as opposed to mixed valence [10,16]. For a smaller left-hand side in Eq. (1) the ground state occurs as predominantly M^{n+}; for a larger left-hand side $M^{(n-1)+}$ dominates the ground state. Distinct ground states are outside the scope of band theory, where the emphasis is only on W_n.

Although in the above competition is assumed between $M^{(n-1)+}$ and M^{n+}, Eq. (1) applies equally, if not even more strongly, to the case where the competition is between $M^{(n-1)+}$ and $M^{(n+1)+}$, as is true for $BaBiO_3$*, where the competition is between* Bi^{3+} *and* Bi^{5+}.

Since $\Delta E_{M,n}$ is nearly independent of the detailed nature of M within a given row of the periodic table, it follows that for *unusually large* I_n oxides will have a strong tendency to be in the ionic state $M^{(n-1)+}$. This conclusion immediately explains the occurrence of only Bi^{3+} in $BaBiO_3$. As shown in Fig. 1, Bi^{3+} with closed-shell configuration ($[Xe]4f^{14}5d^{10}6s^2$) has unusually large ionization energy among the three consecutive p-block elements Pb, Bi, and Po in the periodic table.

As with Bi^{3+}, unusually large nth ionization energy is a characteristic of all closed-shell $M^{(n-1)+}$. Additionally, for systems already close to the boundary of the inequality (1), external variables such as temperature, pressure, or doping can change $\Delta E_{M,n}$ or $\Delta(W)$ enough to lead to first-order transition from open-shell M^{n+} to closed-shell $M^{(n-1)+}$. The most well known among such valence transitions are the temperature, pressure, and light induced neutral-to-ionic transitions in the family of mixed-stack organic charge-transfer solids, which have been known for more than four decades [16]. Reference [10] postulated that exactly such a dopant induced $Cu^{2+} \rightarrow Cu^{1+}$ valence transition occurs at the pseudogap transition in the hole-doped cuprates, and at the antiferromagnet-to-superconductor transition in the electron-doped cuprates. The

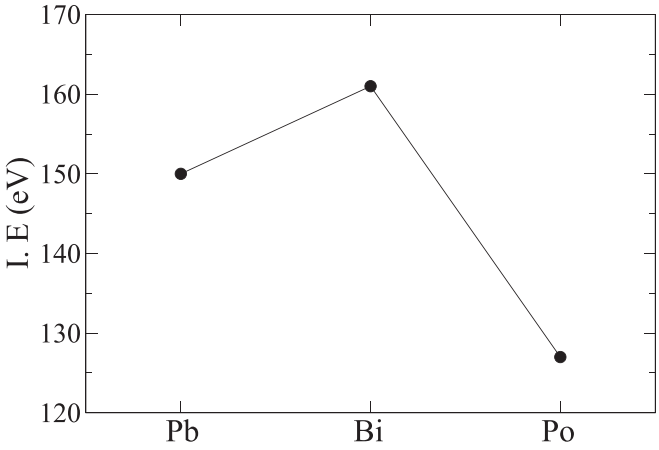

FIG. 1. Fourth ionization energies of Pb, Bi, and Po [61]. The absence of Bi^{5+} in $BaBiO_3$ is due to the exceptional stability of Bi^{3+}. The plot of second ionization energies of $3d$ transition metals shows a similar peak at Cu because of the closed-shell nature of Cu^{1+} [see Fig. 1 in Ref. [10] and Fig. 2(a)].

driving forces behind the transition are the unusually high ionization energy of closed-shell Cu^{1+} with closed-shell electron configuration $3d^{10}$ (see Fig. 1 in Ref. [10]), as well as contribution from $\Delta(W)$ in the doped state. The latter favors the lower ionicity, because of the far greater number of charge carriers in this state.

The charge-transfer gap following the valence transition is the excitation $Cu^{1+}O^{1-} \rightarrow Cu^{2+}O^{2-}$, opposite to the excitation in the undoped semiconducting state, and is therefore "negative." Following valence transition doped cuprates consist of an effective nearly $\frac{1}{4}$-filled O hole band ($\frac{3}{4}$-filled electron band) with the closed-shell Cu^{1+} playing no significant role [10]. The lattice of O ions is frustrated (see Fig. 4). It has been shown from numerically accurate exact diagonalization, quantum Monte Carlo, and path-integral renormalization-group calculations that a density wave of Cooper pairs as well as a superconducting state occur naturally and uniquely within the frustrated $\frac{1}{4}$-filled (and $\frac{3}{4}$-filled) band Hubbard Hamiltonian [57,62,63]. This effective *anion-centric one-band model* can describe both hole- and electron-doped cuprates and, aside from explaining correlated-electron SC, is able to give detailed physical understandings of the spatial broken symmetries in the hole-doped cuprates, the unusual stability of the antiferromagnetic phase in the standard T' compounds, as well as the appearance of SC in undoped thin-film T' cuprates [10].

Closed-shell characters of Cu^{1+} and Bi^{3+} are true independent of crystal structure. In octahedral complexes with large CFSE unusually large ionization energy will be true for cations with electron occupancy of t_{2g}^6. This tendency would be strongest with $5d$ cations with CFSE much larger than for $3d$ and $4d$ cations. Reference [10] therefore proposed that the transition to the pseudogap state in electron-doped Sr_2IrO_4 is a consequence of the valence transition from Ir^{4+} with open-shell configuration t_{2g}^5 to Ir^{3+} with closed-shell t_{2g}^6. As in the cuprates this would again imply a nearly $\frac{1}{4}$-filled oxygen hole band, which would have the tendency to the same charge-ordering and hence the same d-wave-like gap. Strong

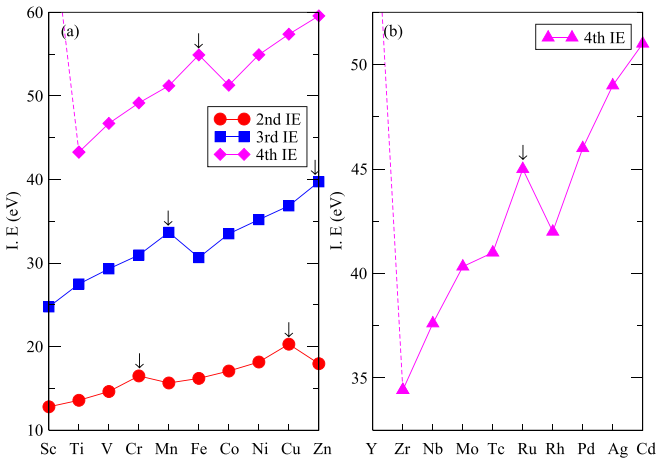

FIG. 2. (a) Second, third, and fourth ionization energies of 3*d* transition metals. Note the local maxima on half-filled ions in each case. (b) Fourth ionization energies of 4*d* transition metals. Both sets of data are from Ref. [61]. The scales along the *y* axes are different in (a) and (b), but the difference in the ionization energies of Ru^{3+} and its immediate neighbors in the periodic table is larger that that between Cu^{1+} and Zn^{1+}.

support for this viewpoint comes from the *known* true charge distribution in octahedral $IrTe_2$. Even as the nominal charges are $Ir^{4+}(Te^{2-})_2$, the true ionic charges are accepted [64,65] to be $Ir^{3+}(Te^{1.5-})_2$.

IV. TYPE-II NEGATIVE CHARGE-TRANSFER GAP: CATIONS WITH HALF-FILLED SHELLS

As seen in the previous section, negative charge transfer is very likely with closed-shell cations and can be driven by both $\Delta E_{m,n}$ and $\Delta(W)$, thereby introducing a new mechanism for IMT. In the following I discuss how a similar IMT can occur in complexes where formal charges correspond to nearly half-filled *d* shells.

A. Unusually large ionization energies of half-filled ions

Beyond completely closed-shell cations, isolated free ions that are exactly half filled also have unusually large ionization energies. For the *d*-block elements this is true for ions with electron configurations d^5, which as free ions occur in their high spin configurations because of Hund's coupling. Figure 2(a) shows that the second ionization energy of of Cr ($Cr^{1+} \rightarrow Cr^{2+} + e$), the third ionization energy of Mn ($Mn^{2+} \rightarrow Mn^{3+} + e$), and the fourth ionization energy of Fe ($Fe^{3+} \rightarrow Fe^{4+} + e$) are all significantly larger than those for similarly charged cations neighboring in the periodic table. The behavior seen in Fig. 2(a) for free ions remains true for octahedral complexes of 3*d* elements where CFSE is weak to moderate and Hund's coupling dominates. Thus octahedral complexes of Mn^{2+} are almost universally high spin, while complexes of Fe^{3+} are often high spin. This cooperative behavior emerges from the close coupling between high ionization energy and Hund's coupling in the 3*d* series. For the same ionic charge CFSE variation is $3d < 4d < 5d$. Thus the much larger 5*d* CFSE dominates over Hund's coupling in Ir, and the closed-shell nature of octahedral Ir^{3+} drives the $Ir^{4+} \rightarrow Ir^{3+}$ transition. Behavior intermediate between 3*d* (where Hund's coupling dominates) and 5*d* (where CFSE dominates) can emerge for 4*d*, as discussed below.

B. Valence transition and negative charge-transfer gap in Sr_2RuO_4

The nominal charge of the Ru ion in Sr_2RuO_4 and Ca_2RuO_4 is Ru^{4+} with four *d* electrons. The ion is assumed to be in the low spin state in all prior theoretical work (two experimental studies have, however, claimed high spin Ru^{4+} in Sr_2RuO_4 [66] and metallic $SrRuO_3$ [67]). Figure 2(b) plots the fourth ionization energies of the 4*d* free elements. As expected, the ionization energy of the isolated Ru^{3+} ion is exceptionally large compared to those of Tc^{3+} and Rh^{3+}, with the differences (4.0 and ≈3 eV, respectively) larger than the difference in the ionization energies of Cu^{1+} and Zn^{1+} (≈2 eV). Should the true charge on the Ru ions in Sr_2RuO_4 be +3 instead of the nominal +4, it would imply that Sr_2RuO_4 lies in the same class of materials as bismuthate, cuprate, and Sr_2IrO_4.

The charge-spin coupling implied in Figs. 2(a) and 2(b) introduces a new mechanism for IMT in d^4-based systems, as presented below. As in the cuprates and bismuthates I compare the relative energies of the Sr_2RuO_4 crystal with Ru ions in charge state Ru^{3+} (hereafter labeled as $|\mathrm{III}\rangle$) versus charge state Ru^{4+} (labeled as $|\mathrm{IV}\rangle$), with the additional condition that the Ru^{3+} ions are assumed to be in the high spin state [further ionization of which is energetically costly as seen in Fig. 2(b)] while the Ru^{4+} ions are low spin.

Beyond the terms already included in Eq. (1), interactions that determine the relative energies of $|\mathrm{III}\rangle$ and $|\mathrm{IV}\rangle$ include $U(\mathrm{CFSE}: j)$, $U(\mathrm{Coulomb}; j)$, and $U(\mathrm{exchange}: j)$, where $|j\rangle = |\mathrm{III}\rangle$ and $|\mathrm{IV}\rangle$, $U(\mathrm{CFSE}: j)$ is the crystal-field stabilization energy, $U(\mathrm{Coulomb}; j)$ is the direct Coulomb repulsion between electrons occupying the *d* orbitals (Hubbard repulsions between electrons occupying the same as well as different *d* orbitals), and $U(\mathrm{exchange}: j)$ is Hund's exchange energy. The inequality that determines the competition between high spin Ru^{3+} and low spin Ru^{4+} is

$$I_n + A_2 + \Delta E_{M,n} + \Delta(W) + \Delta_{\mathrm{CF}} + \Delta_C + \Delta_J \gtrless 0. \quad (2)$$

In the above, $n = 4$ and A_2, $\Delta E_{M,n}$, and $\Delta(W)$ have the same meanings as in Eq. (1). $\Delta_{\mathrm{CF}} = U(\mathrm{CFSE: III}) - U(\mathrm{CFSE: IV})$ is negative [$U(\mathrm{CFSE: III}) \simeq 0$] and favors state $|\mathrm{IV}\rangle$ over state $|\mathrm{III}\rangle$, while $\Delta_J = U(\mathrm{exchange: III}) - U(\mathrm{exchange: IV})$ is positive and favors state $|\mathrm{III}\rangle$ over state $|\mathrm{IV}\rangle$. It is difficult to estimate $\Delta_C = U(\mathrm{Coulomb; III}) - U(\mathrm{Coulomb; IV})$; it is assumed to be small relative to the larger Δ_{CF} and Δ_J, the competition between which determines the relative stabilities of high versus low spin in semiconductors. As with Eq. (1), a smaller (larger) left-hand side favors Ru^{4+} (Ru^{3+}).

The following are now pointed out.

(i) First-principles calculations for the cuprates have consistently determined large direct O-O hoppings $t_{pp} \geqslant 0.5 t_{dp}$ in the cuprates [68,69], where t_{dp} involves the $d_{x^2-y^2}$ orbitals. The t_{dp} in state $|\mathrm{IV}\rangle$, however, involves only the d_{xy} orbitals

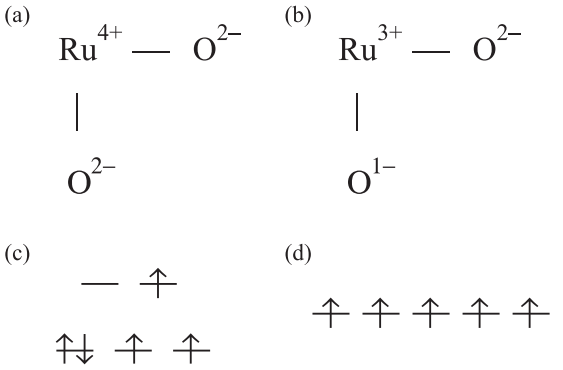

FIG. 3. Schematics of the layer intra-unit-cell charge distributions in (a) insulating Ca_2RuO_4 and (b) metallic Sr_2RuO_4. (c) Schematic of the virtual intermediate state in a current induced (electron-doping induced) ruthenate conductor with an electron added to the low spin Ru^{4+} cation. For strong intraorbital Coulomb repulsion the extra electron occupies an e_g orbital and reduces the CFSE self-consistently, which in turn leads to (d) a stable Ru^{3+} ion in the metallic state with high ionization energy. Charge carriers in the metallic state are entirely on the O ions in this case. Ru^{3+} ions contribute to magnetism but not transport.

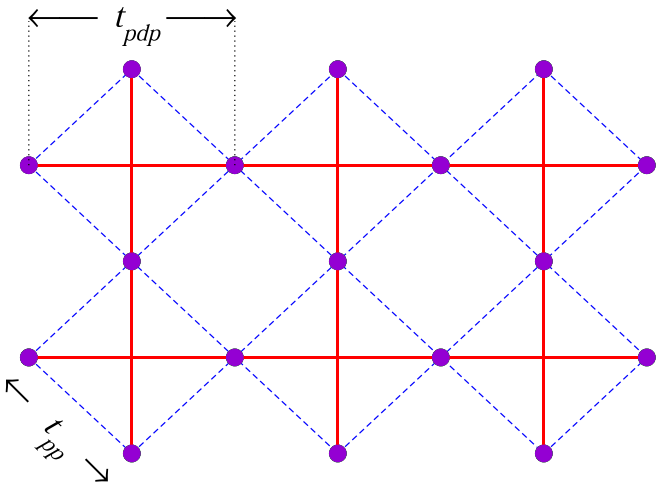

FIG. 4. The checkerboard lattice of O ions, common to both Sr_2RuO_4 and cuprates, in their superconducting states. The half-filled Ru^{3+} (closed-shell Cu^{1+}) cations, which occur at the intersections of the solid lines, are not explicitly shown as they do not play any role in superconductivity, which involves only the $\frac{3}{4}$-filled O band. The nearest-neighbor direct O-O hoppings t_{pp}, as well as the O-O hoppings via the metal cations, t_{pdp} (see text), are shown. The magnitudes of t_{pdp} are the same for O-M-O bond angles of 90° and 180°, and are much larger for cuprates than for Sr_2RuO_4. In the latter it is anticipated that $|t_{pp}| > |t_{pdp}|$ (see text).

and is hence considerably smaller than t_{dp} in the cuprates. On the other hand, it is reasonable to assume that the magnitudes of t_{pp} are similar in the two classes of materials. Significantly enhanced conductivity can therefore occur from direct hopping between O ions, but *only if charge carriers occupy the O sites to begin with.* Correspondingly, a large contribution by $\Delta(W)$ to the stabilization of $|\mathrm{III}\rangle$ with far larger number of charge carriers over $|\mathrm{IV}\rangle$ with few charge carriers on O sites is to be anticipated.

(ii) The actual contribution by $\Delta(W)$ to the stabilization of $|\mathrm{III}\rangle$ is even larger, given that in $|\mathrm{III}\rangle$ t_{dp} includes contributions from the $d_{x^2-y^2}$ orbitals, over and above from d_{xy}.

(iii) Δ_{CF} in Eq. (2) need not be a rigid quantity as in the competition between two semiconductors, where $\Delta(W) = 0$ by default. When the competition is between a semiconductor and a metal it is likely that Δ_{CF} decreases self-consistently with conduction. It is argued in (i) above that conduction due to electron hopping between O ions requires state $|\mathrm{III}\rangle$ to make significant contribution to the electronic structure of Sr_2RuO_4. Given the large Coulomb repulsion between electrons occupying the same d orbital, this implies that the extra electron in the Sr^{3+} ion will likely occupy an e_g orbital [see Fig. 3(c)], which in turn reduces Δ_{CF}, leading to additional occupancy of e_g and finally to the configuration shown in Fig. 3(d).

Based on the above I posit that the difference between the Mott-Hubbard semiconductor bulk Ca_2RuO_4 and metallic Sr_2RuO_4 originates from different charges of the Ru ions in these systems. As a consequence of the negative charge-transfer gap in Sr_2RuO_4 there is a preponderance of layer O^{1-} ions instead of a few due to self-doping. In Figs. 3(a) and 3(b) schematics of the IMT in oxides with large ionization energies of $M^{(n-1)+}$ are shown, while the schematics in Figs. 3(c) and 3(d) refer to the current induced $Ru^{4+} \rightarrow Ru^{3+}$ transition. The difference between Ca_2RuO_4 and Sr_2RuO_4 is ascribed to the much smaller size of the Ca ion leading to much larger Madelung energy stabilization of the high-charge state and hence larger $\Delta E_{M,n}$ for Ca_2RuO_4 in Eq. (2), that favors Ru^{4+}. It is shown in the next section that straightforward explanations of the experimental results presented in Sec. II that are difficult to understand with low spin Ru^{4+} are obtained within the negative charge-transfer gap model in which Ru ions occur as high spin Ru^{3+} which contribute to magnetism but not transport.

V. EXPLANATIONS OF EXPERIMENTS WITHIN THE NEGATIVE CHARGE-TRANSFER GAP MODEL

A. Sr_2RuO_4

1. d-wave SC

Within the valence transition model the charge carriers are entirely on the O ions which have average charge −1.5. The Ru^{3+} ions play at most a virtual role in transport, exactly as the closed-shell Cu^{1+} ions in the cuprates [10]. Figure 4 shows the charge-carrying checkerboard O sublattice of the RuO_2 layer, rotated 45° relative to the Ru-O-Ru bonds. The effective Hamiltonian H_{eff} for the charge carriers on the checkerboard lattice is

$$H_{\mathrm{eff}} = -\sum_{\langle ij\rangle,\sigma} t_{pp}(p^{\dagger}_{i,\sigma}p_{j,\sigma} + \mathrm{H.c.}) - \sum_{[ij],\sigma} t_{pdp}(p^{\dagger}_{i,\sigma}p_{j,\sigma} + \mathrm{H.c.}) + U_p\sum_i n_{pi,\uparrow}n_{pi,\downarrow} \times\frac{1}{2}\sum_{\langle ij\rangle} V_p^{NN} n_{pi}n_{pj} + \frac{1}{2}\sum_{(ij)} V_p^{NNN} n_{pi}n_{pj}. \quad (3)$$

Here $p^{\dagger}_{i,\sigma}$ creates a hole (O^{1-}) on the p orbital of an O^{2-} ion, $n_{pi,\sigma} = p^{\dagger}_{i,\sigma} p_{i,\sigma}$, and $n_p = \sum_{\sigma=\uparrow,\downarrow} n_{pi,\sigma}$. Sums are over the O ions in the RuO_2 layer; $\langle\ \rangle$ denotes nearest-neighbor (NN) oxygens; [ ] denotes O ions linked via the same Ru^{3+} ion (NN and NNN O ions are linked by Ru-O bonds at 90° and 180°, respectively); and ( ) are NNN O ions irrespective of whether they are linked via the same Ru ion or not. U_p, $V_p^{\rm NN}$ and $V_p^{\rm NNN}$ are Coulomb repulsions between pairs of holes on the same NN and NNN p orbitals, respectively. The hopping parameter t_{pp} is the direct hopping between NN O ions while t_{pdp} is the effective hopping between NN and NNN O ions linked by the same Ru^{3+} ion, $t_{pdp} = t_{dp}^2/\Delta E$, t_{dp} is the hopping between a Ru d orbital and oxygen p orbital, and $\Delta E = E(Ru^{4+}O^{2-}) - E(Ru^{3+}O^{1-})$. The large ionization energy of Ru^{3+} implies large ΔE, which is likely to make $|t_{pdp}| < |t_{pp}|$.

Given the $S = 5/2$ spin state of Ru^{3+}, for $t_{pp} = 0$ ferromagnetic spin coupling between $O^{1-} - O^{1-}$ would have been expected. For $|t_{pp}| > |t_{pdp}|$ anticipated here, spin singlet coupling dominates. Sophisticated quantum-mechanical calculations by the present author and colleagues [57,62,63] using exact diagonalization, constrained path quantum Monte Carlo, and path-integral renormalization-group calculations have consistently shown that singlet superconducting pair-pair correlations are uniquely enhanced by the Hubbard interaction (relative to the noninteracting model) at $\frac{3}{4}$ filling and a narrow carrier density region about it on a geometrically frustrated lattice. At all other fillings the Hubbard interaction suppresses the pair-pair correlations relative to the noninteracting ($U_p = V_p^{\rm NN} = V_p^{\rm NNN} = 0$) Hamiltonian, a result that agrees with the conclusions of Ref. [56]. Very recently, Clay and Roy have further shown that again uniquely at this same filling Su-Schrieffer-Heeger bond phonons and the Hubbard U act cooperatively to further enhance the superconducting pair-pair correlation, while no such cooperative interaction is found at any other filling [70].

Correlation-driven SC in the frustrated $\frac{3}{4}$-filled or $\frac{1}{4}$-filled band is *not* due to spin fluctuation. Rather, the superconducting state in the frustrated $\frac{3}{4}$-filled band evolves from a commensurate CDW of Cooper pairs—a paired-electron crystal (PEC)—that is unique to the exactly $\frac{3}{4}$-filled frustrated lattice [71,72]. Beyond cuprates, this theory of correlated-electron SC readily explains the limitation of SC [50,52] to relatively narrow carrier concentration range $0.37 \leqslant x \leqslant 0.5$ in $Ba_{1-x}K_xBiO_3$, for which as of now there exists no other clear explanation. With the Bi ions occurring only as Bi^{3+}, as determined experimentally [50,51] the charge on the O ions ranges from 1.50 to 1.54 for this range of x. The s-wave symmetry here is a natural consequence of the three-dimensional O lattice in $Ba_{1-x}K_xBiO_3$.

2. Muon-spin rotation and apparent time-reversal breaking

The apparent broken time-reversal symmetry is associated with the ferromagnetic Ru^{3+}-Ru^{3+} spin-spin coupling, which, however, is unrelated to the SC itself. This is also the simplest explanation for the invariance of the Josephson critical current under the inversion of current and magnetic fields [25]: SC involves the O ions only and not the Ru ions. It is very likely that the same mechanism of transport applies also to the ferromagnetic metal $SrRuO_3$, which has been thought to be an itinerant ferromagnet. A model-specific prediction is made in the next section.

3. T_c enhancement by the application of uniaxial pressure

Carrier density dependent calculations of superconducting pair-pair correlations have found that these are enhanced relative to the noninteracting Hamiltonian over a region of small width about $\frac{3}{4}$ filling, with the strongest correlations occurring for exactly $\frac{3}{4}$ filling [62,63,73]. The implication for this is that, should the filling be less than exactly $\frac{3}{4}$ [as it should be under ambient pressure, since integral charges require complete reverse charge transfer $Ru^{4+}(O^{2-})_2 \rightarrow Ru^{3+}(O^{2-})_1(O^{1-})_1$], T_c will be less than the maximum possible. Within the valence transition model, pressure along the Ru-O bonds (but not along the Ru-Ru diagonal direction) enhances the reverse charge transfer because of the increase in t_{dp}.

B. Ca_2RuO_4

1. Current induced IMT

There is no explanation of the current induced IMT [18,19] and diamagnetism [36] within the usual models of Mott transition. Within the valence transition model the IMT is driven by the large $\Delta(W)$ within Eq. (2), giving a current-carrying state the structure of which is very different from the insulator (see Fig. 3), with nearly half the O ions occurring as O^{1-}. As mentioned above, the correlated $\frac{3}{4}$-filled geometrically frustrated lattice exhibits a strong tendency to form a commensurate PEC [71,72], with nearest-neighbor spin singlets separated by pairs of vacancies (corresponding to periodic O^{1-}-O^{1-}-O^{2-}-O^{2-}). Reference [10] has pointed out that the charge-ordered state in the cuprates (and many other systems with the same carrier density) can be understood within the same picture. The concept of the PEC is identical to the concept of the density wave of Cooper pairs that has been conjectured by many authors to be proximate to the superconducting state in the cuprates [74–77]. With increased frustration, the PEC gives way to a paired-electron liquid and ultimately to a superconductor [62,63,73]. The diamagnetism in the current-driven semimetallic state in Ca_2RuO_4 is ascribed to the paired-electron liquid, in agreement with prior explanation by the author of the low-temperature Nernst effect measurements in cuprates [10].

2. La doping, IMT, and ferromagnetism

The valence transition model gives the simplest explanation for the IMT induced by La doping, as illustrated in Figs. 3(c) and 3(d). The extra electron initially occupies an e_g orbital. Undoped Ca_2RuO_4 is already very close to instability, and the smallest perturbation leads to a first-order transition. The ferromagnetism detected at small dopings [20] is due to the ferromagnetic couplings between the high spin Ru ions, which, as mentioned above, also explains the muon spin experiments in Sr_2RuO_4.

3. Coappearance of ferromagnetism and possible SC

This also has a natural explanation within the negative charge-transfer gap model. Observation of SC here is reminiscent of superconductivity in undoped thin-film T' cuprates, which is readily understood with the negative charge-transfer gap model [10]. Due to the reduced $\Delta E_{M,n}$ in thin films, the charge-transfer gap is naturally negative in these compounds. Reduced $\Delta E_{M,n}$ is also true in nanocrystals of Ca_2RuO_4 and the L as opposed to S crystal structure is evidence for the same. Ferromagnetism driving SC, as claimed in Ref. [21], is a consequence of the requirement that SC can occur only when the Ru ions are in the trivalent state. The magnetism and the SC, however, involve two different components of the nanocrystal.

VI. EXPERIMENTAL PREDICTIONS

Here I make experimental predictions specific to the negative charge-transfer gap model.

A. Charge densities on the layer oxygens in Sr_2RuO_4

^{17}O NMR experiments should be able to find the charge densities on the layer oxygens. It is predicted that this charge density in Sr_2RuO_4 in the superconducting state is -1.5.

B. Intra-unit-cell inequivalency of layer oxygens

It is conceivable that in the current induced semimetallic state, or in weakly La-doped $CaRu_2O_4$, intra-unit-cell inequivalency of layer O ions will be detected by ^{17}O NMR or other experiments, as in the case of $YBa_2Cu_3O_y$ [42,45].

C. Spin susceptibility due to Ru ions

As of writing Knight-shift measurements have been repeated only for the O sites [7,8]. The earlier literature also reported extensive measurements of Ru-ion spin susceptibility through T_c. ^{99}Ru Knight-shift measurement with the magnetic field parallel to the RuO_2 layer [78] and ^{101}Ru Knight-shift measurements with the field perpendicular to the layer [79] both showed that the spin susceptibility due to Ru ions remained unchanged below T_c. *It is predicted that these observations will continue to be the same, in spite of the* ^{17}O *NMR measurements.* If found to be true this will be the strongest proof that the Ru ions do not participate in normal-state transport and SC in Sr_2RuO_4.

VII. CONCLUSIONS

In conclusion, nominal and true charges in conducting perovskite oxides can be very different. The natural state of oxide ions is not necessarily O^{2-}, even though that is commonly assumed. The second electron affinity of O is positive (it costs energy to add the second extra electron) and it is only the gain in Madelung energy in the insulating oxides that drives a metal oxide to a state with high cation charge M^{n+} and anion charge O^{2-}. With cations that in their lower charge state $M^{(n-1)+}$ have high ionization energies, IMT occurs via a valence transition $M^{n+} \rightarrow M^{(n-1)+}$, which in the quasi-2D materials leaves the layers with a $\frac{3}{4}$-filled oxygen band of electrons. Average charge of -1.5 on oxygen anions is neither strange nor unprecedented—this is, for example, the known true charge on the oxygens in alkali-metal sequioxides X_4O_6, $X =$ Rb, Cs [80–82].

The negative charge-transfer gap model gives the simplest yet most comprehensive explanations for the many apparently peculiar observations in Sr_2RuO_4 and Ca_2RuO_4. All of the peculiarities are understood once it is recognized that magnetism and SC involve two entirely different components of the crystals: the high spin Ru^{3+} ions are responsible for the magnetic behavior but the charge carriers are entirely on the O sites. The two phenomena are, however, coupled in that it is the lower charge on the cation that gives the specific carrier density on the oxygen sites necessary for correlated-electron SC. Additional attractive features of the theory are that the model appears to be simultaneously applicable to many other correlated-electron systems [10] and is supported by numerical calculations of superconducting pair-pair correlations [57,62,63,70].

Note added in Proof. Based on quasiparticle interference imaging, a recent paper [9] has suggested $d_{x^2-y^2}$ superconducting gap symmetry for Sr_2RuO_4, which would be in agreement with the conclusion of the present paper, even as the theoretical modeling in this paper is based on the usual Ru-centric multiband model of superconducivity.

ACKNOWLEDGMENTS

The author acknowledges support from NSF Grant No. CHE-1764152 and is grateful to Dr. R. Torsten Clay (Mississippi State University), Dr. Charles Stafford (University of Arizona), and Dr. Shufeng Zhang (University of Arizona) for their careful readings of the paper and suggestions. The author also acknowledges close interactions and collaborations through the years with Dr. Clay.

[1] A. P. Mackenzie and Y. Maeno, The superconductivity of Sr_2RuO_4 and the physics of spin-triplet pairing, Rev. Mod. Phys. **75**, 657 (2003).

[2] A. P. Mackenzie, T. Scaffidi, C. W. Hicks, and Y. Maeno, Even odder after twenty-three years: The superconducting order parameters puzzle of Sr_2RuO_4, npj Quantum Mater. **2**, 40 (2017).

[3] C. W. Hicks, D. O. Brodsky, E. A. Yelland, A. S. Gibbs, J. A. N. Bruin, M. E. Barber, S. D. Edkins, K. Nishimura, S. Yonezawa, Y. Maeno, and A. P. Mackenzie, Strong increase of T_c of Sr_2RuO_4 under both tensile and compressive strain, Science **344**, 283 (2014).

[4] H. Taniguchi, K. Nishimura, S. K. Goh, S. Yonezawa, and Y. Maeno, Higher-T_c superconducting phase in Sr_2RuO_4 induced by in-plane uniaxial pressure, J. Phys. Soc. Jpn. **84**, 014707, (2015).

[5] A. Steppke, L. Zhao, M. E. Barber, T. Scaffidi, F. Jerzembeck, H. Rosner, A. S. Gibbs, Y. Maeno, S. H. Simon, A. P. Mackenzie, and C. W. Hicks, Strong peak in T_c of Sr_2RuO_4 under uniaxial pressure, Science **355**, eaaf9398 (2017).

[6] E. Hassinger, P. Bourgeois-Hope, H. Taniguchi, S. R. de Cotret, G. Grissonnanche, M. S. Anwar, Y. Maeno, N. Doiron-Leyraud, and L. Taillefer, Vertical Line Nodes in the Superconducting Gap Structure of Sr_2RuO_4, Phys. Rev. X **7**, 011032 (2017).

[7] Y. Luo *et al.*, Normal State ^{17}O NMR Studies of Sr_2RuO_4 Under Uniaxial Stress, Phys. Rev. X **9**, 021044 (2019).

[8] A. Pustogow, Yongkang Luo, A. Chronister, Y.-S. Su, D. A. Sokolov, F. Jerzembeck, A. P. Mackenzie, C. W. Hicks, N. Kikugawa, S. Raghu, E. D. Bauer, and S. E. Brown, Constraints on the superconducting order parameter in Sr_2RuO_4 from oxygen-17 nuclear magnetic resonance, Nature (London) **574**, 72 (2019).

[9] R. Sharma, S. D. Edkins, Z. Wang, A. Kostina, C. Sow, Y. Maeno, A. P. Mackenzie, J. C. Seamus Davis, and V. Madhavan, Momentum-resolved superconducting energy gaps of Sr_2RuO_4 from quasiparticle interference imaging, Proc. Natl. Acad. Sci. USA **117**, 5222 (2020).

[10] S. Mazumdar, Valence transition model of the pseudogap, charge order, and superconductivity in electron-doped and hole-doped copper oxides, Phys. Rev. B **98**, 205153 (2018).

[11] A. de la Torre, S. McKeown Walker, F. Y. Bruno, S. Ricco, Z. Wang, I. Gutierrez Lezama, G. Scheerer, G. Giriat, D. Jacard, C. Berthod, T. K. Kim, M. Hoesch, E. C. Hunter, R. S. Perry, A. Tamai, and F. Baumberger, Collapse of the Mott Gap and Emergence of a Nodal Liquid in Lightly Doped Sr_2IrO_4, Phys. Rev. Lett. **115**, 176402 (2015).

[12] Y. H. Kim, N. H. Sung, J. D. Denlinger, and B. J. Kim, Observation of a *d*-wave gap in electron-doped Sr_2IrO_4, Nat. Phys. **12**, 37 (2016).

[13] I. Battisti, K. M. Bastiaans, V. Fedoseev, A. de la Torre, N. Iliopoulos, A. Tamai, E. C. Hunter, R. S. Perry, J. Zaanen, F. Baumberger, and M. P. Allan, Universality of pseudogap and emergent order in lightly doped Mott insulators, Nat. Phys. **13**, 21 (2017).

[14] J. B. Torrance, J. E. Vazquez, J. J. Mayerle, and V. Y. Lee, Discovery of a Neutral-To-Ionic Phase-Transition in Organic Materials, Phys. Rev. Lett. **46**, 253 (1981).

[15] S. Kosihara, Y. Tokura, T. Mitani, G. Saito, and T. Koda, Photoinduced valence instability in the organic molecular compound tetrathiafulvalene-p-chloranil, Phys. Rev. B **42**, 6853 (1990).

[16] M. Masino, N. Castagnetti, and A. Girlando, Phenomenology of the neutral-ionic valence instability in mixed stack charge-transfer crystals, Crystals **7**, 108 (2017).

[17] G. W. Scheerer, Z. Ren, S. Watanabe, G. Lapertot, D. Aoki, D. Jaccard, and K. Miyake, The dominant role of critical valence fluctuations on high t_c superconductivity in heavy fermions, npj Quantum Mater. **3**, 41 (2018).

[18] F. Nakamura, M. Sakaki, Y. Yamanaka, S. Tamaru, T. Suzuki, and Y. Maeno, Electric-field-induced metal maintained by current of the Mott insulator Ca_2RuO_4, Sci. Rep. **3**, 2536 (2013).

[19] R. Okazaki, Y. Nishina, Y. Yasui, F. Nakamura, T. Suzuki, and I. Terasaki, Current-induced gap suppression in the the Mott insulator Ca_2RuO_4, J. Phys. Soc. Jpn. **82**, 103702 (2013).

[20] C. Cao, S. McCall, V. Dobrosavljevic, C. S. Alexander, J. E. Crow, and R. P. Guertin, Ground-state instability of the Mott insulator Ca_2RuO_4: Impact of light la doping on the metal-insulator transition and magnetic ordering, Phys. Rev. B **61**, R5053 (2000).

[21] H. Nobukane, K. Yanagihara, Y. Kunisada, Y. Ogasawara, K. Isono, K. Nomura, K. Tanahashi, T. Nomura, T. Akiyama, and S. Tanda, Co-appearance of superconductivity and ferromagnetism in a Ca_2RuO_4 nanofilm crystal, Sci. Rep. **10**, 3462 (2020).

[22] K. Ishida, H. Mukuda, Y. Kitaoka, K. Asayama, Z. Q. Mao, Y. Mori, and Y. Maeno, Spin-triplet superconductivity in Sr_2RuO_4 identified by ^{17}O Knight shift, Nature (London) **396**, 658 (1998).

[23] G. M. Luke, Y. Fudamoto, K. M. Kojima, M. I. Larkin, J. Merrin, B. Nachumi, Y. J. Uemura, Y. Maeno, Z. Q. Mao, Y. Mori, H. Nakamura, and M. Sigrist, Time-reversal symmetry-breaking superconductivity in Sr_2RuO_4, Nature (London) **394**, 558 (1998).

[24] J. Xia, Y. Maeno, P. T. Beyersdorf, M. M. Fejer, and A. Kapitulnik, High Resolution Polar Kerr Effect Measurements of Sr_2RuO_4: Evidence for Broken Time-Reversal Symmetry in the Superconducting State, Phys. Rev. Lett. **97**, 167002 (2006).

[25] S. Kashiwaya, K. Saitoh, H. Kashiwaya, M. Koyanagi, M. Sato, K. Yada, Y. Tanaka, and Y. Maeno, Time-reversal invariant superconductivity of Sr_2RuO_4 revealed by Josephson effects, Phys. Rev. B **100**, 094530 (2019).

[26] H. Karapetyan, M. Hücker, G. D. Gu, J. M. Tranquada, M. M. Fejer, J. Xia, and A. Kapitulnik, Magneto-Optical Measurements of a Cascade of Transitions in Superconducting $La_{1:875}Ba_{0:125}CuO_4$ Single Crystals, Phys. Rev. Lett. **109**, 147001 (2012).

[27] V. Grinenko *et al.*, Split superconducting and time-reversal symmetry-breaking transitions, and magnetic order in Sr_2RuO_4 under uniaxial stress, arXiv:2001.08152v2.

[28] S. Yonezawa, T. Kajikawa, and Y. Maeno, First-Order Superconducting Transition of Sr_2RuO_4, Phys. Rev. Lett. **110**, 077003 (2013).

[29] M. Braden, G. André, S. Nakatsuji, and Y. Maeno, Crystal and magnetic structure of Ca_2RuO_4: Magnetoelastic coupling and the metal-insulator transition, Phys. Rev. B **58**, 847 (1998).

[30] O. Friedt, M. Braden, G. André, P. Adelmann, S. Nakatsuji, and Y. Maeno, Structural and magnetic aspects of the metal-insulator transition in $Ca_{2-x}Sr_xRuO_4$, Phys. Rev. B **63**, 174432 (2001).

[31] H. Fukazawa and Y. Maeno, Filling control of the Mott insulator Ca_2RuO_4, J. Phys. Soc. Jpn. **70**, 460 (2001).

[32] S. Nakatsuji, V. Dobrosavljević, D. Tanasković, M. Minakata, H. Fukazawa, and Y. Maeno, Mechanism of Hopping Transport in Disordered Mott Insulators, Phys. Rev. Lett. **93**, 146401 (2004).

[33] A. Liebsch and H. Ishida, Subband Filling and Mott Transition in $Ca_{2-x}Sr_xRuO_4$, Phys. Rev. Lett. **98**, 216403 (2007).

[34] E. Gorelov, M. Karolak, T. O. Wehling, F. Lechermann, A. I. Lichtenstein, and E. Pavarini, Nature of the Mott transition in Ca_2RuO_4, Phys. Rev. Lett. **104**, 226401 (2010).

[35] F. Nakamura, T. Goko, M. Ito, T. Fujita, S. Nakatsuji, H. Fukazawa, Y. Maeno, P. Alireza, D. Forsythe, and S. R. Julian, From Mott insulator to ferromagnetic metal: A pressure study of Ca_2RuO_4, Phys. Rev. B **65**, 220402(R) (2002).

[36] C. Sow, S. Yonezawa, S. Kitamura, T. Oka, K. Kuroki, F. Nakamura, and Y. Maeno, Current-induced strong diamagnetism in the Mott insulator Ca_2RuO_4, Science **358**, 1084 (2017).

[37] K. Fúrsich, J. Bertinshaw, P. Butler, M. Krautloher, M. Minola, and B. Keimer, Raman scattering from current-stabilized nonequilibrium phases in Ca_2RuO_4, Phys. Rev. B **100**, 081101(R) (2019).

[38] J. W. Zhang *et al.*, Nano-Resolved Current-Induced Insulator-Metal Transition In the Mott Insulator Ca_2RuO_4, Phys. Rev. X **9**, 011032 (2019).

[39] J. Bertinshaw, N. Gurung, P. Jorba, H. Liu, M. Schmid, D. T. Mantadakis, M. Daghofer, M. Krautloher, A. Jain, G. H. Ryu, O. Fabelo, P. Hansmann, G. Khaliullin, C. Pfleiderer, B. Keimer, and B. J. Kim, Unique Crystal Structure of Ca_2RuO_4 in the Current Stabilized Semimetallic State, Phys. Rev. Lett. **123**, 137204 (2019).

[40] H. Zhao, B. Hu, F. Ye, C. Hoffmann, I. Kimchi, and G. Cao, Nonequilibrium orbital transitions via applied electrical current in calcium ruthenates, Phys. Rev. B **100**, 241104(R) (2019).

[41] M. Naito, Y. Krockenberger, A. Ikeda, and H. Yamamoto, Reassessment of the electronic state, magnetism, and superconductivity in high-T_c cuprates with the Nd_2CuO_4 structure, Physica C **523**, 28 (2016).

[42] T. Wu, H. Mayaffre, S. Kraemer, M. Horvatić, C. Berthier, W. N. Hardy, L. Ruixing, D. A. Bonn, and M.-H. Julien, Incipient charge order observed by NMR in the normal state of $YBa_2Cu_3O_y$, Nat. Commun. **6**, 6438 (2015).

[43] Y. Kohsaka, T. Hanaguri, M. Azuma, M. Takano, J. C. Davis, and H. Takagi, Visualization of the emergence of the pseudogap state and the evolution to superconductivity in a lightly hole-doped Mott insulator, Nat. Phys. **8**, 534 (2012).

[44] R. Comin, R. Sutarto, F. He, E. H. D. S. Neto, L. Chauviere, A. Frano, R. Liang, W. N. Hardy, D. A. Bonn, Y. Yoshida, H. Eisaki, A. J. Achkar, D. G. Hawthorn, B. Keimer, G. A. Sawatzky, and A. Damascelli, Symmetry of charge order in cuprates, Nat. Mater. **14**, 796 (2015).

[45] S. Reichardt, M. Jurkutat, R. Guehne, J. Kohlrautz, A. Erb, and J. Haase, Proof of bulk charge ordering in the CuO_2 plane of the cuprate superconductor $YBa_2Cu_3O_{6.9}$ by high pressure NMR, Condens. Matter **3**, 23 (2018).

[46] N. P. Armitage, P. Fournier, and R. L. Greene, Progress and perspectives on electron-doped cuprates, Rev. Mod. Phys. **82**, 2421 (2010).

[47] E. H. D. S. Neto, R. Comin, F. He, R. Sutarto, Y. Jiang, R. L. Greene, G. A. Sawatzky, and A. Damascelli, Charge ordering in the electron-doped $Nd_{2-x}Ce_xCuO_4$, Science **347**, 282 (2015).

[48] E. H. D. S. Neto, B. Yu, M. Minola, R. Sutarto, E. Schierle, F. Boschini, M. Zonno, M. Bluschke, J. Higgins, Y. Li, G. Yu, E. Weschke, F. He, M. Le Tacon, R. L. Greene, M. Greven, G. A. Sawatzky, B. Keimer, and A. Damascelli, Doping-dependent charge order correlations in electron-doped cuprates, Sci. Adv **2**, e1600782 (2016).

[49] T. M. Rice and L. Sneddon, Real Space Electron Pairing in $BaPb_{1-x}Bi_xO_3$, Phys. Rev. Lett. **47**, 689 (1981).

[50] N. C. Plumb, D. J. Gawryluk, Y. Wang, Z. Ristic, J. Park, B. Q. Lv, Z. Wang, C. E. Matt, N. Xu, T. Shang, K. Conder, J. Mesot, S. Johnston, M. Shi, and M. Radovic, Momentum-Resolved Electronic Structure of the High-T_c Superconductor Parent Compound $BaBiO_3$, Phys. Rev. Lett. **117**, 037002 (2016).

[51] A. Khazraie, K. Foyevtsova, I. Elfimov, and G. A. Sawatzky, Oxygen holes and hybridization in the bismuthates, Phys. Rev. B **97**, 075103 (2018).

[52] S. Pei, J. D. Jorgensen, B. Dabrowski, D. G. Hinks, D. R. Richards, and A. W. Mitchell, Structural phase diagram of the $Ba_{1-x}K_xBiO_3$ system, Phys. Rev. B **41**, 4126 (1990).

[53] B. J. Kim, H. Jin, S. J. Moon, J.-Y. Kim, B.-G. Park, C. S. Leem, J. Yu, T. W. Noh, C. Kim, S.-J. Oh, J.-H. Park, V. Durairaj, G. Cao, and E. Rotenberg, Novel $J_{\rm eff} = 1/2$ Mott State Induced by Relativistic Spin-Orbit Coupling in Sr_2IrO_4, Phys. Rev. Lett. **101**, 076402 (2008).

[54] Y. J. Yan, M. Q. Ren, H. C. Xu, B. P. Xie, R. Tao, H. Y. Choi, N. Lee, Y. J. Choi, T. Zhang, and D. L. Feng, Electron-Doped Sr_2IrO_4: An Analogue of Hole-Doped Cuprate Superconductors Demonstrated by Scanning Tunneling Microscopy, Phys. Rev. X **5**, 041018 (2015).

[55] M. Hashimoto, I. M. Vishik, R.-H. He, T. P. Devereaux, and Z.-X. Shen, Energy gaps in the high-transition temperature cuprate superconductors, Nat. Phys. **10**, 483 (2014).

[56] C.-M. Chung M. Qin, H. Shi, E. Vitali, C. Hubig, S. R. White U. Schollöck, and S. Zhang, Absence of superconductivity in the pure two-dimensional Hubbard model, arXiv:1910.08931.

[57] N. Gomes, W. Wasanthi, De Silva, T. Dutta, R. T. Clay, and S. Mazumdar, Coulomb enhanced superconducting pair correlations in the frustrated quarter-filled band, Phys. Rev. B **93**, 165110 (2016).

[58] Z. G. Soos and S. Mazumdar, Neutral-ionic interface in organic charge-transfer salts, Phys. Rev. B **18**, 1991 (1978).

[59] N. Nagaosa and J. Takimoto, Theory of neutral-ionic transition in organic crystals, 1. Monte-Carlo simulation of modified Hubbard model, J. Phys. Soc. Jpn. **55**, 2735 (1986).

[60] Y. Anusooya-Pati, Z. G. Soos, and A. Painelli, Symmetry crossover and excitation thresholds at the neutral-ionic transition of the modified Hubbard model, Phys. Rev. B **63**, 205118 (2001).

[61] See www.webelements.com

[62] W. Wasanthi De Silva, N. Gomes, S. Mazumdar, and R. T. Clay, Coulomb enhancement of superconducting pair-pair correlations in a 3/4-filled model for κ-(BEDT-TTF)$_2$X, Phys. Rev. B **93**, 205111 (2016).

[63] R. T. Clay and S. Mazumdar, From charge- and spin-ordering to superconductivity in the organic charge-transfer solids, Phys. Rep. **788**, 1 (2019).

[64] Y. S. Oh, J. J. Yang, Y. Horibe, and S.-W. Cheong, Anionic Depolymerization Transition in $IrTe_2$, Phys. Rev. Lett. **110**, 127209 (2013).

[65] A. F. Fang, G. Xu, T. Dong, P. Zheng, and N. L. Wang, Structural phase transition in $IrTe_2$: A combined study of optical spectroscopy and band structure calculations, Sci. Rep. **3**, 1153 (2013).

[66] M. Itoh, M. Shikano, and T. Shimura, High- and low-spin transition of Ru^{4+} in the perovskite-related layered system $Sr_{n+1}Ru_nO_{3n+1}$, $n = 1$, 2, and ∞ with changes in n, Phys. Rev. B **51**, 16432 (1995).

[67] A. J. Grutter, F. J. Wong, E. Arenholz, A. Vailionis, and Y. Suzuki, Evidence of high-spin Ru and universal magnetic anisotropy in $SrRuO_3$ thin films, Phys. Rev. B **85**, 134429 (2012).

[68] M. Hirayama, Y. Yamaji, T. Misawa, and M. Imada, *Ab initio* effective Hamiltonians for cuprate superconductors, Phys. Rev. B **98**, 134501 (2018).

[69] M. Hirayama, T. Misawa, T. Ohgoe, Y. Yamaji, and M. Imada, Effective Hamiltonian for cuprate superconductors derived

from multiscale ab initio scheme with level renormalization, Phys. Rev. B **99**, 245155 (2019).

[70] R. T. Clay and D. Roy, Cooperative enhancement of superconducting correlations by electron-electron and electron-phonon interactions in the quarter-filled band, Phys. Rev. Research **2**, 023006 (2020).

[71] H. Li, R. T. Clay, and S. Mazumdar, The paired-electron crystal in the two-dimensional frustrated quarter-filled band, J. Phys.: Condens. Matter **22**, 272201 (2010).

[72] S. Dayal, R. T. Clay, H. Li, and S. Mazumdar, Paired electron crystal: Order from frustration in the quarter-filled band, Phys. Rev. B **83**, 245106 (2011).

[73] N. Gomes, R. T. Clay, and S. Mazumdar, Absence of superconductivity and valence bond order in the Hubbard-Heisenberg model for organic charge-transfer solids, J. Phys.: Condens. Matter **25**, 385603 (2013).

[74] M. Franz, Crystalline electron pairs, Science **305**, 1410 (2004).

[75] H.-D. Chen, O. Vafek, A. Yazdani, and S.-C. Zhang, Pair Density Wave in the Pseudogap State of High Temperature Superconductors, Phys. Rev. Lett. **93**, 187002 (2004).

[76] Z. Tesanovic, Charge Modulation, Spin Response, and Dual Hofstadter Butterfly in High-T_c Cuprates, Phys. Rev. Lett. **93**, 217004 (2004).

[77] M. H. Hamidian, S. D. Edkins, S. H. Joo, A. Kostin, H. Eisaki, S. Uchida, M. J. Lawler, E.-A. Kim, A. P. Mackenzie, K. Fujita, J. Lee, and J. C. Davis, Detection of a Cooper-pair density wave in $Bi_2Sr_2CaCu_2O_{8+x}$, Nature (London) **532**, 343 (2016).

[78] K. Ishida, H. Mukuda, Y. Kitaoka, Z. Q. Mao, H. Fukazawa, and Y. Maeno, Ru NMR probe of spin susceptibility in the superconducting state of Sr_2RuO_4, Phys. Rev. B **63**, 060507(R) (2001).

[79] K. Ishida, H. Murakawa, H. Mukuda, Y. Kitaoka, Z. Q. Mao, and Y Maeno, NMR and NQR studies on superconducting Sr_2RuO_4, J. Phys. Chem. Solids **69**, 3108 (2008).

[80] P. Adler *et al.*, Verwey-type charge ordering transition in an open-shell p-electron compound, Sci. Adv. **4**, eaap7581 (2018).

[81] R. H. Colman, H. E. Okur, W. Kockelmann, C. M. Brown, S. Annette, C. Felser, M. Jansen, and K. Prassides, Elusive valence transition in mixed-valence sesquioxide Cs_4O_6, Inorg. Chem. **58**, 14532 (2019).

[82] T. Knaflic *et al.*, Spin-dimer ground state driven by consecutive charge and orbital ordering transitions in the anionic mixed-valence compound Rb_4O_6, Phys. Rev. B **101**, 024419 (2020).